Accurate measurement of guided modes in a plate using a bidirectional approach

Ludovic Moreau, Jean-Gabriel Minonzio, Josquin Foiret, Emmanuel Bossy, Maryline Talmant, Pascal Laugier

To cite this version:

Ludovic Moreau, Jean-Gabriel Minonzio, Josquin Foiret, Emmanuel Bossy, Maryline Talmant, et al.. Accurate measurement of guided modes in a plate using a bidirectional approach. Journal of the Acoustical Society of America, 2014, 135 (1), pp.EL15. 10.1121/1.4832335 . hal-01394313

HAL Id: hal-01394313
https://hal.sorbonne-universite.fr/hal-01394313

Accurate measurement of guided modes in a plate using a bidirectional approach.

Ludovic Moreau[1,2], Jean-Gabriel Minonzio[1,2], Josquin Foiret[1,2], Emmanuel Bossy[3], Maryline Talmant[1,2], and Pascal Laugier[1,2]

[1]UPMC Univ Paris 06, UMR 7623, LIP, F-75005, Paris, France

[2]CNRS, UMR 7623, Laboratoire d'Imagerie Paramétrique, F-75006, Paris, France

[3]Institut Langevin ESPCI ParisTech, CNRS UMR 7587, INSERM ERL U979, 10 rue Vauquelin F-75005 Paris France

ludovic.moreau@upmc.fr, jean-gabriel.minonzio@upmc.fr, josquin.foiret@upmc.fr, emmanuel.bossy@espci.fr, maryline.talmant@upmc.fr, pascal.laugier@upmc.fr

Abstract

Measuring guided wave propagation in long bones is of interest to the medical community. When an inclination exists between the probe and the tested specimen surface, a bias is introduced on the guided mode wavenumbers. The aim of this study was to generalize the bidirectional axial transmission technique initially developed for the first arriving signal. Validation tests were performed on academic materials such a bone-mimicking plate covered with either a silicon or fat-mimicking layer. We show the wavenumbers measured with the probe parallel to the waveguide surface can be obtained by averaging the apparent wavenumbers measured in two opposite directions.

July 29th 2013

PACS numbers 43.60.Fg, 43.35 Cg, 43.80.Vj, 43.20.Ye, 43.20.Mv,

Running title: bidirectional approach for guided modes

1. Introduction

Recent studies showed that the cortical shell of long bones supports the propagation of ultrasonic guided waves (GW).[1] Because ultrasonic GW are sensitive to the elastic and geometrical properties of the waveguide, they may be used to estimate important biomarkers of the biomechanical competence of bone, such as cortical thickness[2, 3] or stiffness[4] itself related to cortical porosity.[5] This is of significant interest to the medical community because these bone properties (*i.e.*, cortical thickness and porosity) are known determinants of bone strength. Their measurement could improve skeletal status assessment.

Several axial transmission techniques have been proposed to measure ultrasound propagation in long bones. While in most studies investigators have focused attention on the measurement of the velocity of the earliest component of the signal recorded at the receivers, the so-called first arriving signal (FAS),[1] several studies in the past decade reported approaches to measure different signal components, such as the fundamental flexural GW,[3, 6, 7] or higher order GW dispersion curves.[8, 9] In particular, measuring GW frequency-dependent wavenumbers is expected to provide a more complete view of the biomechanical status of bone compared to FAS velocity measurements alone. From the measurements of GW propagation, the geometrical and elastic properties can be recovered by (*i*) post-processing the signals to obtain the corresponding frequency-dependent wavenumbers, and (*ii*) inverting these data by fitting of an appropriate waveguide model. The present work focuses on the measurement and post-processing of the signals, in order to produce reliable wavenumber data prior to the inversion process. In this purpose, an ultrasonic array, placed in contact on top of the outer soft tissue layer, is used in combination with specific signal processing.[10] However, the corresponding measurements can be biased by the presence of soft tissue[11, 12] In particular, variations of soft tissue thickness along the receiving array implies a phase shift in the recorded signals, which translates directly on the apparent wavenumbers and ultimately on the estimates of the above-mentioned bone properties.

Such variations of soft tissue thickness may occur *in vivo* when the probe is placed onto the skin at skeletal sites such as the forearm either because the skin thickness may be heterogeneous or because the pressure under the probe may be uneven. With only one direction measured, a proper compensation for the phase shifts in the signals would require an a priori knowledge of the soft tissue velocity and the angle between the probe and the bone, which is difficult in a clinical sequence of measurements using current axial transmission techniques. Consequently the so-called bidirectional axial transmission approach, an alternative method that was first introduced in the measurement of FAS velocity,[13] is generalized here to GW. In its original context, the method consisted of evaluating the time-of-flight of the FAS in two opposite directions, and computing the harmonic mean of the two sets of data in order to cancel the effect of soft tissue without the need to know the soft tissue thickness characteristics. Bossy *et al*. reported that, while uncompensated FAS velocity values could be biased by more than 10% for an inclination of a few degrees between the test specimen surface and the probe, the bidirectional compensation procedure reduced the bias on velocity measurement to a relative precision error lower than 0.2 - 0.3 %.[13] The bidirectional correction of the FAS velocity has been applied in clinical studies.[14, 15]

The impact of a variation of the thickness of soft tissue along the length of the bone on the GW wavenumbers has not been investigated so far. The aim of this paper was to generalize the bidirectional correction to GW measurements. Validation tests were performed on academic materials such a bone-mimicking plate covered with either a silicon or fat-mimicking layer to approximate the effects of soft tissue.

2. Principle of the bidirectional approach

Measurement of GW propagating in cortical bone is affected by the presence of soft tissue between the probe and the bone, particularly when a lack of parallelism between the receivers and the bone surface modifies the phase differences between the different signals. Consequently, although the intrinsic wavenumbers in the bone are not changed, the apparent wavenumbers measured with the probe are modified. This was quantified for the first time for FAS measurement.[13]

Consider a waveguide immersed in an ambient fluid (Fig.1).[16] The bidirectional approach described below assumes that the considered waves are guided along the (Ox_3) direction, but the approach does not depend on the exact type of waveguide (free elastic plate, bilayer model, cylindrical waveguide …). The n^{th} guided mode of wavenumber k_n radiates in the surrounding fluid at the critical angle θ_n according to Snells-Descartes law

$$\sin(\theta_n) = \frac{k_n}{k_{\mathrm{F}}}, \qquad (1)$$

where k_{F} is the wavenumber of the longitudinal wave in the fluid, and θ_n is defined relatively to (Ox_3) as shown in Figure 1. The angle β, resulting from the variation of the soft tissue thickness along the probe, measures the inclination between the receiver array and the test specimen surface (Fig.1). The receivers are aligned along the ($O'r$) axis. With basic trigonometric manipulations, the phase difference $\Delta\phi_{ij}$ between the i^{th} and the j^{th} receiver, located at r_i and r_j, writes as $K_n \, \|r_i r_j\|$, with K_n the apparent wavenumber given by

$$K_n = k_n \cos(\beta)\left(1 + \frac{\tan(\beta)}{\tan(\theta_n)}\right). \qquad (2)$$

For a positive angle β, *i.e.*, the situation depicted on Figure 1, for a transmitting array placed on the right-hand side of the receivers, the apparent wavenumber K_n overestimates the “true” wavenumber k_n, *i.e.*, along the (Ox_3) direction ($\beta = 0°$). From now, $\beta = 0°$ will be referred to as the "parallel case". Reciprocally, it can easily be shown that a transmitting array placed on the left-hand side of the receivers would now lead to underestimate the wavenumber of the considered guided mode. According to Eq. (2) the average between the apparent wavenumbers $K_n^{(1)}$ and $K_n^{(2)}$ measured in both directions yields

$$\frac{K_n^{(1)} + K_n^{(2)}}{2} = k_n\,, \qquad (3)$$

if one considers the first-order Taylor series expansion with respect to β, for small angles. Eq. (3) means that, by assuming homogenous bone properties in the bone portion covered by the probe, an unbiased estimate of the wavenumber k_n of a given guided mode measured in the parallel case can be achieved by simply averaging the apparent wavenumbers $K_n^{(1)}$ and $K_n^{(2)}$ measured on a unique receiving array of the considered guided mode propagating in two opposite directions. Furthermore, Eq. (3) indicates that the soft tissue compensation can be achieved and that k_n can be estimated without the need to know the soft tissue characteristics (velocity, density, angle for instance) under the assumption that they are constant. In conclusion, while the bidirectional correction method has been successfully applied to *in vivo* measurements of the FAS[14, 15] the experimental proof of its validity for GW would be an important step for future developments of guided mode axial transmission measurements of cortical bone.

3. Material and method

To validate the bidirectional correction described above, measurements were performed on two different test samples referred to hereinafter as T1 and T2,: a 4 mm thick bone-mimicking plate covered by a 10 mm thick silicon layer (T1) or a 2 mm thick fat-mimicking layer (T2). The angle β between the probe and the plate was varied with a specially designed goniometer between −2° and +2°, with increments of 0.5°, by applying an uneven pressure onto the soft layer. The investigated range of angular values is typical of that encountered *in vivo*. The silicon has a bulk compression speed of 1230 m.s^{-1} and an attenuation coefficient of about 1 dB.cm^{-1} at 1 MHz.[11] The fat-mimicking layer used here was purchased from CIRS, Norfolk, VA (USA), and has a bulk compression speed of 1430 m.s^{-1} and an attenuation coefficient equal to 0.9 dB.cm^{-1}.MHz^{-1}. The bone-mimicking plate is made of glass fibers embedded in epoxy (Sawbones Pacific Research Laboratories, Vashon, WA, USA).

The axial transmission setup is composed of an ultrasonic probe (Vermon, Tours, France), a multi-channel array controller (Althaïs Technology, Tours, France) and a graphic interface for real-time visualization of the calculated $(f-k)$ diagrams, where f and k are the frequency and the wavenumber, respectively. The probe (Fig.1) contains two groups of five transmitters surrounding a single group of 24 receivers in the center, with a pitch of 0.8 mm. Each emitter is excited with 1 MHz central frequency wideband pulses (−6 dB power spectrum spanning the frequency range of 0.5 to 1.6 MHz). Signals are recorded at a sampling frequency of 20 MHz and a 12-bit resolution. The signals corresponding to all transmit-receive pairs in the array are captured. The probe is placed in contact with the soft-tissue mimicking layer using an ultrasound gel (Aquasonic, Parker Labs, Inc, Fairfield, NJ, USA) to ensure a good coupling, without affecting the measurement.

The wavenumbers of the guided modes were obtained by applying a specific time-space to frequency-wavenumber transform to the temporal signals.[10] This transform involves a classical temporal Fourier transform combined with a projection of test vectors in the signal subspace. In practice, the test vectors are projected onto the basis of the singular vectors of the signals, obtained from the singular value decomposition (SVD) of the transfer matrix. Compared to a classical time-space 2D Fourier transform, this signal-processing method significantly enhances the measured $(f-k)$ diagrams. First, the SVD allows separation of signal from noise. Second, the appropriate choice of normalized projection vectors returns (f – k) values scaled between 0 and 1.

4. Results and discussion

The two above-mentioned tested configurations are representative of the extreme values of soft tissue thickness that can be encountered in different individuals and correspond to a large (resp. short) soft tissue propagation path of the order of ten (resp. two) wavelengths, corresponding respectively to T2 and T1. The experimental wavenumbers *vs*. frequency, $K_n^{(1)}$ (red squares) and $K_n^{(2)}$ (blue circles), measured for T1 and for a 2° inclination of the probe are represented on Fig. 2 and compared to the case of the probe parallel to the bone-mimicking surface, *i.e.* $\beta = 0°$ (black continuous line). Measurements in direction “1” (red squares), achieved with a positive angle β corresponding to the transmitting array placed on the right-hand side of the receivers as illustrated on Fig. 1, are associated to an overestimate of the wavenumbers. The opposite direction “2” (blue circles) is associated to underestimated wavenumbers. The black crosses representing the average of $K_n^{(1)}$ and $K_n^{(2)}$ [Eq. (3)] are in good agreement with the parallel case. This demonstrates that the proposed bidirectional correction, applied to guided mode measured with an angle ($\beta \neq 0°$), provides accurate estimates of the dispersion curve measured in the parallel case ($\beta = 0°$). In order to further illustrate the validity of bidirectional correction for guided waves, such as given by equation (3), the wavenumbers measured in the parallel case (black lines) were transformed following equation (2) with $\beta = +2°$ (dashed red lines) and –2° (dash dot blue lines). The agreement between these predicted biased values and the measured wavenumbers $K_n^{(1)}$ and $K_n^{(2)}$ confirms the validity of our simple compensation approach.

While figure 2 represents the measured wavenumbers for a fixed angle β, figure 3 illustrates, as a function of the angle β, the evolution of (i) the experimental values $K_n^{(1)}$ (red squares) and $K_n^{(2)}$ (blue circles) together with the average value of $K_n^{(1)}$ and $K_n^{(2)}$ (black crosses) and (ii) their corresponding predicted values using Eq. (2) (dashed lines) and Eq. (3) (continuous line) for three particular fixed frequencies [marked with a black circles on Fig. 2(a)]: 0.5 MHz, 0.85 MHz, and 1.75 MHz. The good agreement between predicted and experimental data again confirms the ability of the bidirectional compensation to provide angle-independent estimates of parallel case wavenumbers.. The linear relationship observed for a given frequency in figure 3 between the angle and the wavenumbers is due to the fact that angle β is small, and therefore in Eq. (2), the terms cos(β) and tan(β) can be approximated at the first order by 1 and β respectively.

The second test case (T2) with a much narrower 2mm fat-mimicking layer is shown in figure 4. As for test case T1, the angle-related bias is cancelled when the bidirectional correction is applied, as evidenced from the good agreement between the corrected ($f-k$) values and the wavenumbers measured in the parallel case. The good and similar results obtained for both test cases T1 and T2 shows that the bidirectional correction is valid regardless of the thickness and material properties of the overlaying media For example, it was recently observed that a fluid-like layer inserted between a bone-mimicking plate and the ultrasonic probe resulted in the measurements of additional modes (*i.e.* the guided modes of the inserted fluid-like layer) and in a branching effect between modes propagating in the fluid-like and in the solid waveguides.[11] We hypothesize that the slightly scalloping behavior of the modes presented in figure 2(a) is caused by such an effect. Nevertheless, a good correspondence was obtained between experimental corrected wavenumbers and values obtained for the parallel case. Predicting the dispersion curves by use for instance of a bilayer waveguide model is out of the scope of this letter and will be taken into account in further studies in order to interpret the observed dispersion curves.

The results presented above on laboratory data were obtained from a homogeneous bone-mimicking plate covered with a homogeneous soft tissue mimicking layer. They suggest that the bidirectional modality is efficient to correct the bias caused on GW wavenumbers by a probe inclination. The specific relevance of the approach for clinical measurements needs, however, to be carefully investigated. Some potential complicating experimental factors not directly accounted for in the experiments described here are the heterogeneity and general complexity of cortical bone and soft tissue. From our earlier successful experience where the bidirectional correction was applied to the clinical investigation of the FAS,[14] we believe the correction applicable *in vivo* and might in future studies be shown to be of diagnostic value.

5. Conclusion

This work demonstrates that the bidirectional approach, initially developed for the first arriving signal, can be generalized to guided waves. In this case, the bidirectional correction consists in averaging the apparent frequency-dependent wavenumbers measured in two opposite directions, for each frequency and for each guided mode. These averaged wavenumbers are equivalent to those obtained with the probe parallel to the waveguide surface. Thus, the bias induced on frequency-dependent guided mode wavenumbers by an inclination angle between the probe and the tested specimen can be corrected efficiently, without the prior knowledge of the properties of the intermediate layer between the probe and the surface of the specimen. This is an important contribution for future *in vivo* measurements for which the soft tissue thickness varies along the probe. While the present experiments were specifically designed to mimic bone inspection, the proposed correction may be applied in the nondestructive testing context with non-contact measurements.

Acknowledgments

This work was supported by ANR grant COSTUM 09-TECS-005-03 (2009-2012)

References

1. M. Talmant, J. Foiret, and J. G. Minonzio, *Bone Quantitative ultrasound Chap. 7 Guided waves in cortical bones* (Springer, New York, 2010).
2. X. J. Song, D. A. Ta, and W. Q. Wang, "Analysis of Superimposed Ultrasonic Guided Waves in Long Bones by the Joint Approximate Diagonalization of Eigen-Matrices Algorithm," Ultrasound Med. Biol. **37**, 1704-1713 (2011).
3. P. Moilanen, P. H. F. Nicholson, V. Kilappa, S. L. Cheng, and J. Timonen, "Assessment of the cortical bone thickness using ultrasonic guided waves: Modelling and in vitro study," Ultrasound Med. Biol. **33**, 254-262 (2007).
4. F. Lefebvre, Y. Deblock, P. Campistron, D. Ahite, and J. J. Fabre, "Development of a new ultrasonic technique for bone and biomaterials in vitro characterization," J. Biomed. Mat. Res. **63**, 441-446 (2002).
5. M. Granke, Q. Grimal, A. Saïed, P. Nauleau, F. Peyrin, and P. Laugier, "Change in porosity is the major determinant of the variation of cortical bone elasticity at the millimeter scale in aged women," Bone **49**, 1020-1026 (2011).
6. K. L. Xu, D. A. Ta, and W. Q. Wang, "Multiridge-Based Analysis for Separating Individual Modes From Multimodal Guided Wave Signals in Long Bones," IEEE Trans. Ultrason. Ferroelectr. Freq. Control **57**, 2480-2490 (2010).
7. V. Kilappa, K. Xu, P. Moilanen, E. Heikkola, D. Ta, and J. Timonen, "Assessment of the Fundamental Flexural Guided Wave in Cortical Bone by an Ultrasonic Axial-Transmission Array Transducer," Ultrasound Med. Biol. **39**, 1223-1232 (2013).

8. V. C. Protopappas, D. I. Fotiadis, and K. N. Malizos, "Guided ultrasound wave propagation in intact and healing long bones," Ultrasound Med. Biol. **32**, 693-708 (2006).

9. D. Ta, W. Q. Wang, Y. Y. Wang, L. H. Le, and Y. Q. Zhou, "Measurement of the Dispersion and Attenuation of Cylindrical Ultrasonic Guided Waves in Long Bone," Ultrasound Med. Biol. **35**, 641-652 (2009).

10. J. G. Minonzio, J. Foiret, M. Talmant, and P. Laugier, "Impact of attenuation on guided mode wavenumber measurement in axial transmission on bone mimicking plates," J. Acoust. Soc. Am. **130**, 3574–3582 (2011).

11. J. A. Chen, J. Foiret, J. G. Minonzio, M. Talmant, Z. Q. Su, L. Cheng, and P. Laugier, "Measurement of guided mode wavenumbers in soft tissue-bone mimicking phantoms using ultrasonic axial transmission," Phys. Medi. Biol. **57**, 3025-3037 (2012).

12. P. Moilanen, M. Talmant, V. Kilappa, P. Nicholson, S. L. Cheng, J. Timonen, and P. Laugier, "Modeling the impact of soft tissue on axial transmission measurements of ultrasonic guided waves in human radius," J. Acoust. Soc. Am. **124**, 2364-2373 (2008).

13. E. Bossy, M. Talmant, M. Defontaine, F. Patat, and P. Laugier, "Bidirectional axial transmission can improve accuracy and precision of ultrasonic velocity measurement in cortical bone: A validation on test materials," IEEE Trans. Ultrason. Ferroelectr. Freq. Control **51**, 71-79 (2004).

14. M. Talmant, S. Kolta, C. Roux, D. Haguenauer, I. Vedel, B. Cassou, E. Bossy, and P. Laugier, "In Vivo Performance Evaluation of Bi-Directional Ultrasonic Axial Transmission for Cortical Bone Assessment," Ultrasound Med. Biol. **35**, 912-919 (2009).

15. P. Moilanen, M. Maatta, V. Kilappa, L. Xu, P. H. F. Nicholson, M. Alen, J. Timonen, T. Jamsa, and S. Cheng, "Discrimination of fractures by low-frequency axial transmission ultrasound in postmenopausal females," Ost. Int. **24**, 723-730 (2013).

16. M. F. M. Osborne and S. D. Hart, "Transmission, Reflection, and Guiding of an Exponential Pulse by a Steel Plate in Water. I. Theory," J. Acoust. Soc. Am. **17**, 1-18 (1945).

Figure captions

Figure1. Illustration of the bidirectional probe consisting of one receiving array placed between two transmitting arrays denoted “1” and “2”. The differences of propagation path between the i^{th} and the j^{th} receiver, located at r_i and r_j, are marked with thick lines.

Figure 2. (color online): experimental wavenumbers vs. frequency $K_n^{(1)}$ (squares) and $K_n^{(2)}$ (circles) obtained for a 4 mm thick bone-mimicking plate covered by a 10 mm thick silicone layer (T1). The inclination β of the probe with respect to the bone-mimicking surface is 2°. The black crosses represent the average of $K_n^{(1)}$ and $K_n^{(2)}$. The continuous lines represent the case of the probe parallel to the bone-mimicking surface, *i.e.* $\beta = 0°$. The parallel case wavenumbers are transformed following equation (2) with $\beta = +2°$ (dashed red lines) and –2° (dash dot blue lines).

Figure 3 (color online): Variation, as a function of the angle β, of (i) the experimental values $K_n^{(1)}$ (squares) and $K_n^{(2)}$ (circles) together with the average value of $K_n^{(1)}$ and $K_n^{(2)}$ (crosses) and (ii) their corresponding predicted values using Eq. (2) (dashed lines) and Eq. (3) (continuous line) for three particular modes at fixed frequencies obtained with sample (T1)., marked with a black circles on Fig. 2: 0.5 MHz, 0.85 MHz, and 1.75 MHz.

Figure 4 (color online): same as Fig. 2(a), but for the 4 mm thick bone-mimicking plate covered by a 2 mm thick fat-mimicking layer (T2).

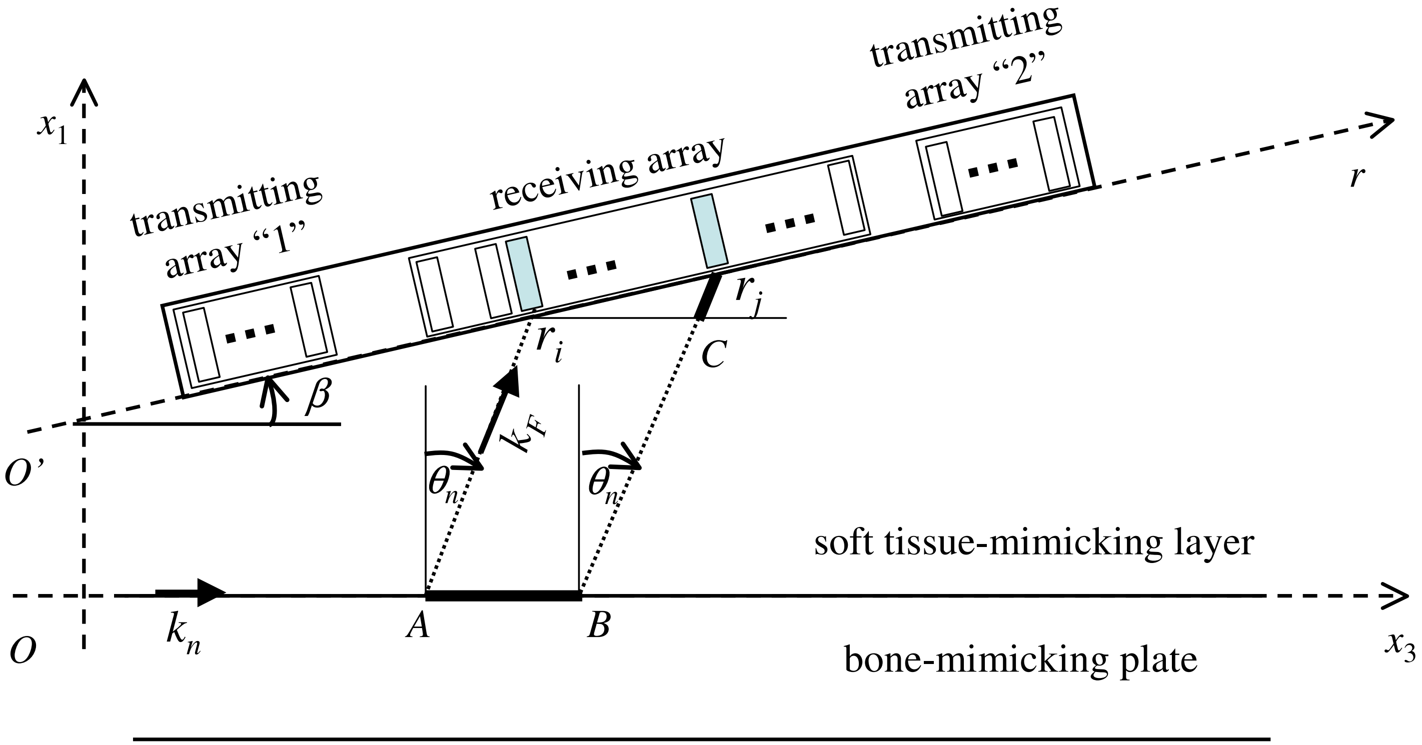

transmitting array "2"
receiving array
transmitting array "1"
x_1
r
r_j
r_i
C
β
O'
k_F
θ_n
θ_n
soft tissue-mimicking layer
k_n
A
B
O
x_3
bone-mimicking plate

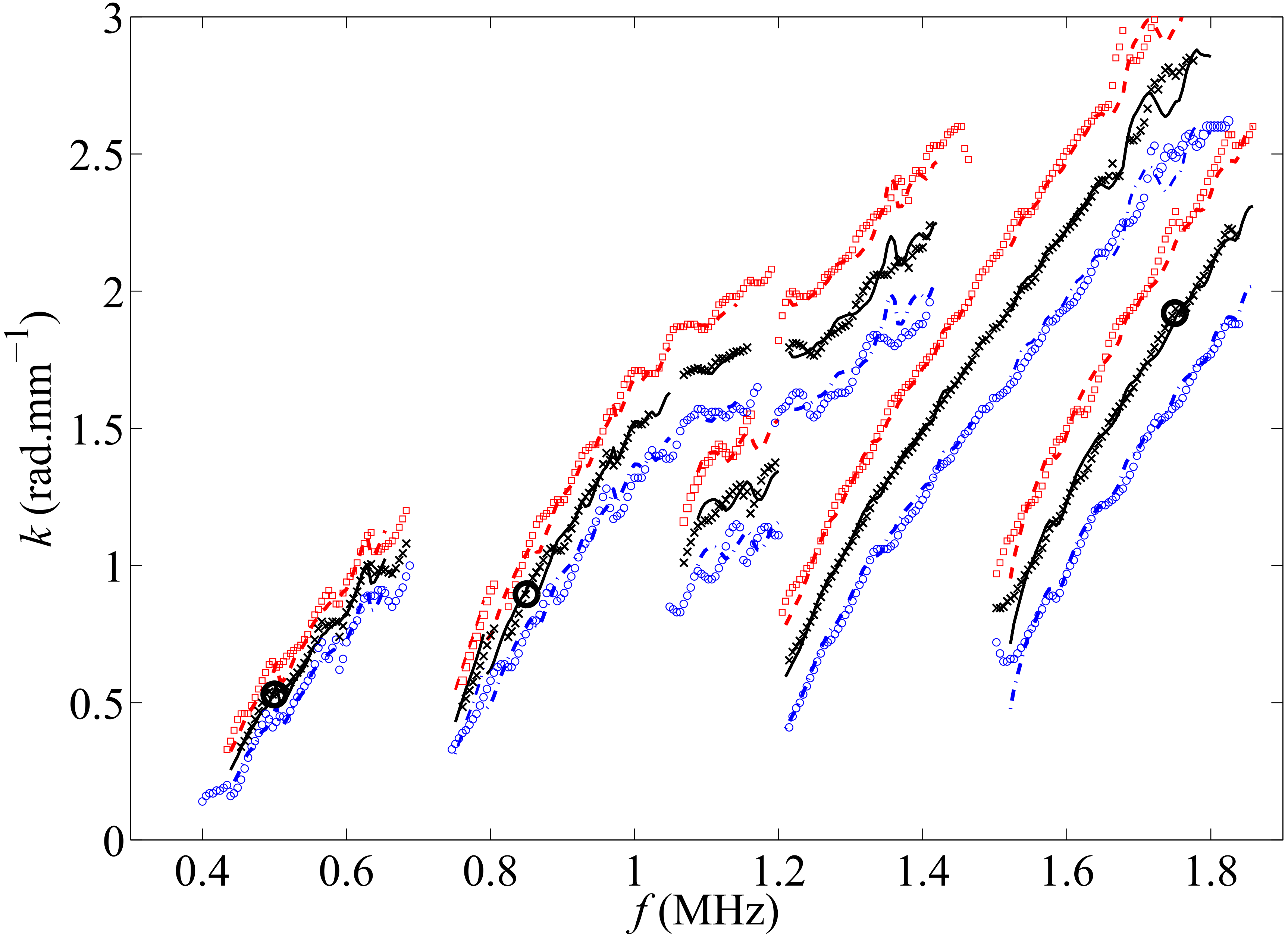

k (rad.mm^{-1})
0
0.5
1
1.5
2
2.5
3
0.4
0.6
0.8
1
1.2
1.4
1.6
1.8
f (MHz)

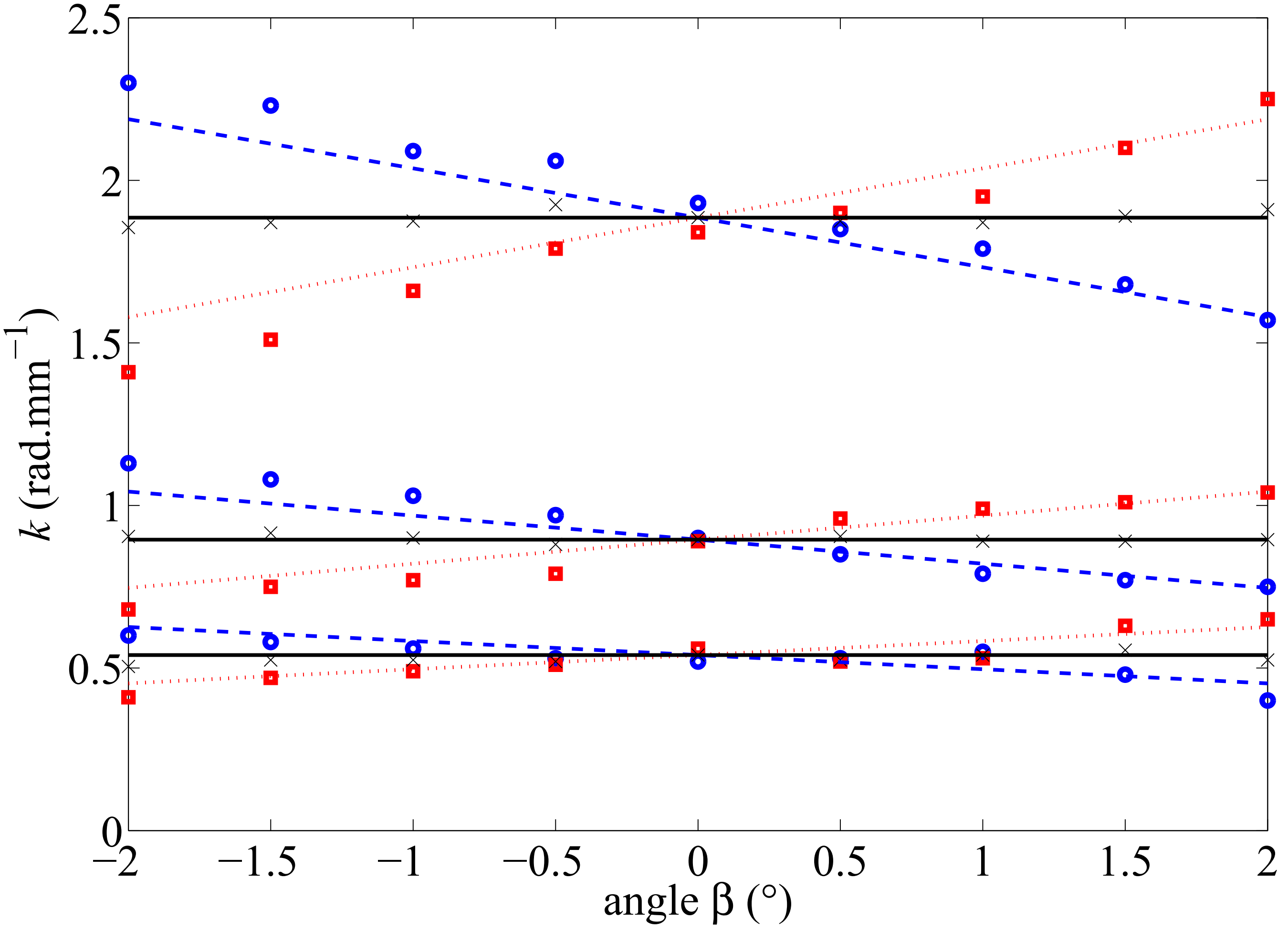
2.5
2
1.5
1
0.5
0
−2
−1.5
−1
−0.5
0
0.5
1
1.5
2
angle β (°)
k (rad.mm^{-1})

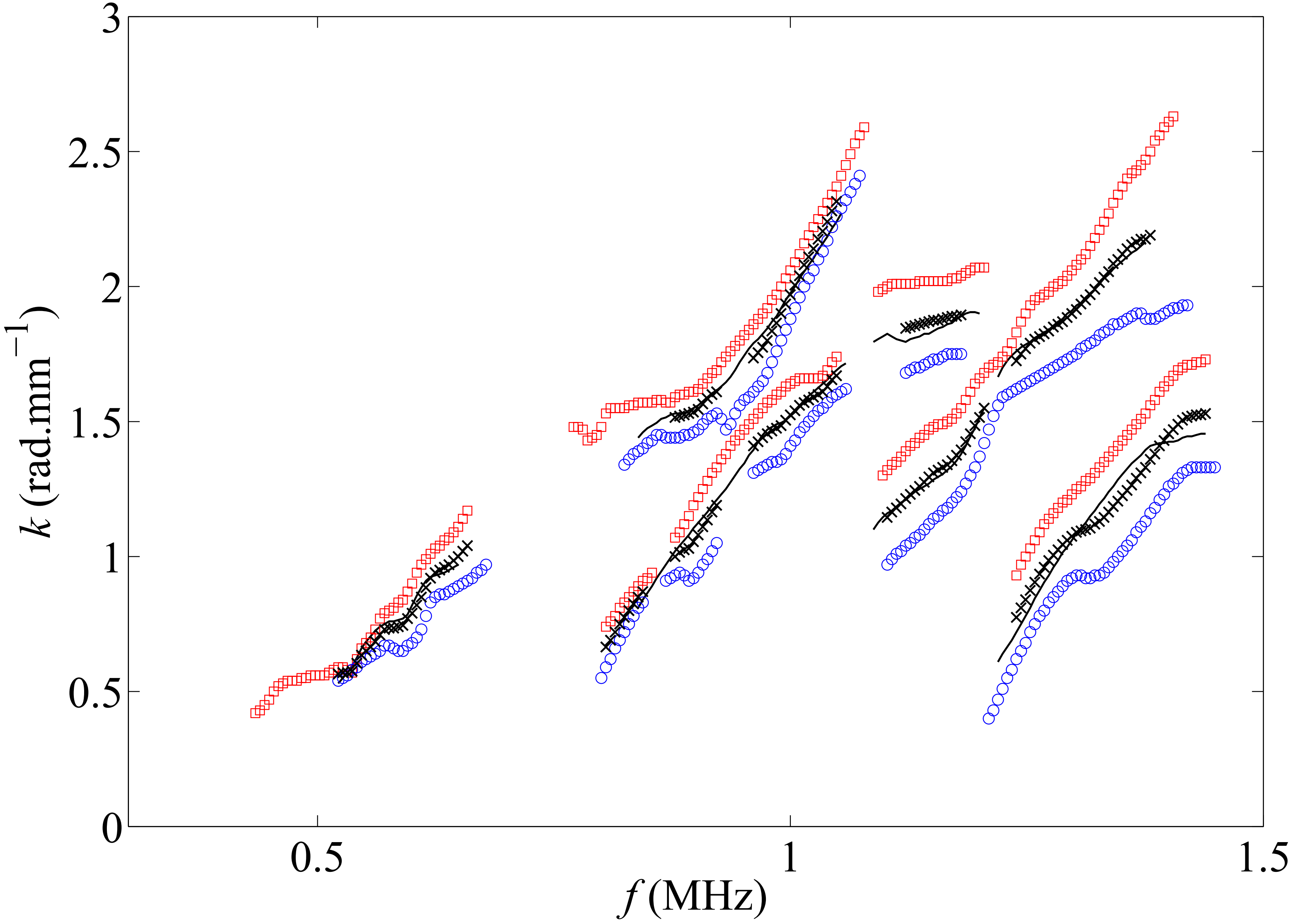
3
2.5
2
1.5
1
0.5
0
k (rad.mm^{-1})
0.5
1
1.5
f (MHz)